Hyperfine-Structure Constants and g_J Values of $^5I_{4,5,6,7,8}$ Atomic States of ^{143,145}Nd†

W. J. Childs and L. S. Goodman
Argonne National Laboratory, Argonne, Illinois 60439
(Received 19 June 1972)

The atomic-beam magnetic-resonance technique has been used to extend the hyperfine-structure and g-value results of Smith and Spalding to all five members of the $4f^46s^2\,{}^5I$ ground multiplet of ^{143,145}Nd. The eigenvectors derived by Conway and Wybourne by fitting the excitation energies are reasonably consistent with the new data. The extent to which the hfs is affected by small components in the eigenvectors is investigated. Empirical values for the radial integrals that appear in the hyperfine structure are compared with predictions based on nonrelativistic Hartree-Fock and on relativistic Hartree-Fock-Slater calculations. The empirical value found for the dipole integral least susceptible to distortion by configuration interaction is within (1–3)% of the value calculated relativistically. Differences between theory and experiment are substantial for some of the other integrals, however. The values of the electric-quadrupole moments of ^{143,145}Nd are found to be $-0.56(6)$ b and $-0.29(3)$ b, respectively.

I. INTRODUCTION

A. History

The atomic energy levels of Nd I have been of interest to atomic spectroscopists for some years. Early papers by Schuurmans[1] and Hassan[2] established most of the lower levels. More recent work by Blaise *et al.*[3] has considerably extended knowledge of the level structure of both odd- and even-parity configurations. Spectroscopic values of the g factors were obtained in several of these investigations. Smith and Spalding[4] obtained more accurate g factors for several of the lowest ^5I states by applying the atomic-beam magnetic-resonance technique to the even-A isotopes. In theoretical treatments, Judd and Lindgren[5] and Conway and Wybourne[6] made least-squares fits to the observed level energies and thereby obtained eigenvectors for the ^5I levels of $4f^46s^2$. They then calculated the g values to be expected, including spin-orbit-mixing, relativistic, and diamagnetic effects, and showed that the predicted values agreed relatively well with the experimental ones. Spalding[7] then extended the atomic-beam investigations to the stable odd-A isotopes ^{143,145}Nd and measured the hyperfine structure (hfs) constants in the $^5I_4$ atomic ground state for both isotopes, and in the $^5I_5$ metastable state of ^{145}Nd in addition. Good values for the ratios of the nuclear moments, and approximate values of the moments themselves, were thereby established. Finally, Smith and Unsworth[8] measured the nuclear magnetic-dipole moments of ^{143,145}Nd directly, using the atomic-beam triple-resonance method.

B. Motivation for Present Experiment

The present experiment[9] can be viewed as a logical extension of that of Spalding[7] on the hfs of the odd-A isotopes ^{143,145}Nd. While the first experiment succeeded in obtaining important information on the nuclear moments, the present work is directed toward investigation of atomic-structure problems. Thus, measurement of the hfs constants and g values for the five members of the ^5I term makes possible a sensitive test of the theory of the J dependence of such observables. It is desirable to view the excitation energy, g factor, magnetic-dipole hfs constant A, and electric-quadrupole hfs constant B as four independent observables of an atomic state, and a single eigenvector should be consistent with all the information. The procedure is to see to what extent the eigenvectors determined from fits to the excitation energies are consistent with the other three observables. The radial integrals that arise in the theory of hfs have recently been calculated relativistically[10,11] for Nd I, and it was of interest to compare these with the values found empirically.

II. EXPERIMENTAL CONSIDERATIONS

A. Apparatus

The apparatus used for the present investigation is a conventional Rabi-type atomic-beam magnetic-resonance machine[12]; the gradients of the inhomogeneous magnetic fields point in the same direction, as proposed by Zacharias.[13] The apparatus has been described before,[14] as has the electronic data-handling system[15] used to make possible the observation of transitions in weakly populated metastable states in the presence of a strong background.

Briefly, beam atoms are ionized by electron bombardment, and subsequently mass analyzed and detected with an electron multiplier, amplifier, and scaler system. The counts from the detector are fed to a multichannel scaler. A clock based on a quartz crystal advances (and resets, as required) the channel address of the scaler in syn-

chronism with a stepwise sweep of the rf used to induce transitions. The sweep can be repeated indefinitely, and a digital noise filter[16] prevents nonrandom noise bursts from harming data that have been accumulating over a long period. It is believed that it is the sensitivity of the data-handling technique that has made possible measurements in the metastable $^5I_8$ state of ^{143,145}Nd; the efficiency of the electron-bombardment ionizer itself is poor—it probably ionizes less than one atom out of 10^4 passing through the detector.

The beam source was a cylindrical oven, $\frac{1}{2}$ in. in diameter and $\frac{3}{4}$ in. high, with a 6.3×0.3-mm slit. A sharp-lipped inner crucible, also of tantalum, was used to limit creep of molten Nd. The oven was heated by electron bombardment until an adequate beam was observed (at about 1500 °C). The homogeneous "C" magnetic field was calibrated by observing resonances in an auxiliary ^{39}K atomic beam from a separate oven.

B. General Principles

The transitions that are observed with the atomic-beam magnetic-resonance technique are normally within individual states of definite electronic angular momentum $\vec{J}$. The appropriate Hamiltonian for the problem is the sum of the hyperfine operator $\mathcal{H}_{hfs}$ and the Zeeman operator $\mathcal{H}_z$; it may be written[17]

$$\mathcal{H}=hA\vec{I}\cdot\vec{J}+hBQ_{op}+hC\Omega_{op}+g_J\mu_B H(J_z+\gamma I_z), \quad (1)$$

where A, B, and C are the magnetic-dipole, the electric-quadrupole, and the magnetic-octupole hyperfine-interaction constants, respectively; g_J is the electron g factor for the atomic state; μ_B is the Bohr magneton; J_z and I_z are the field projections of the electronic and nuclear angular-momentum operators $\vec{J}$ and $\vec{I}$, respectively; $\gamma \ll 1$ is the ratio of the nuclear to the electronic g factors, both in Bohr magnetons; and H is the external magnetic field. The electric-quadrupole and magnetic-octupole operators for a state of definite J may be expressed[17] as

$$Q_{op}=[2I(2I-1)J(2J-1)]^{-1}[\tfrac{3}{2}\vec{I}\cdot\vec{J}(2\vec{I}\cdot\vec{J}+1) - I(I+1)J(J+1)], \quad (2)$$

$$\Omega_{op}=5[4I(I-1)(2I-1)J(J-1)(2J-1)]^{-1}\{8(\vec{I}\cdot\vec{J})^3 + 16(\vec{I}\cdot\vec{J})^2+\tfrac{8}{5}(\vec{I}\cdot\vec{J})[-3I(I+1)J(J+1) + I(I+1)+J(J+1)+3]-4I(I+1)J(J+1)\}. \quad (3)$$

In calculating matrix elements of Eq. (1), it may be noted that

$$\langle JIFM\,|\,\vec{I}\cdot\vec{J}\,|\,JIFM\rangle=\tfrac{1}{2}[F(F+1)-I(I+1)-J(J+1)]. \quad (4)$$

In the absence of a magnetic field ($H=0$), the eigenvalues of Eq. (1) may be characterized by the total-angular-momentum quantum number F (associated with $\vec{F}=\vec{I}+\vec{J}$) and by its z projection M. In a magnetic field, F is no longer a good quantum number, but the zero-field representation is often retained for convenience; each state becomes a linear combination of the zero-field basis states of pure F. When a transition is observed at a frequency ν, the transition energy $h\nu$ is the difference between the appropriate pairs of eigenvalues of Eq. (1).

C. Procedure

Table I lists the excitation energies[3] of the various members of the $4f^46s^2\,{}^5I$ ground multiplet of Nd I; all other atomic states lie higher. The relative number of atoms in a magnetic substate of each level is also given for isotopes 142, 143, and 145 for the approximate beam-source temperature of 1500 °C. It can be seen that hfs experiments, which are possible only for the less-abundant odd-A isotopes 143 and 145, will be more difficult than Zeeman experiments on the even-A isotope ^{142}Nd, and that measurements on any isotope will be very difficult for the higher metastable states.

Using even-even isotopes, Smith and Spalding[4] were able to obtain rough values for the g factors of the states $^5I_{4,5,6,7}$ but were unable to detect any atoms in the $^5I_8$ state. The first part of the present experiment was carried out to refine and extend their measurements. Since there is no hfs in the even-A isotopes of Nd, the resonance frequency for a transition is proportional to the magnetic field, which was precisely calibrated by observing resonances in an auxiliary beam of ^{39}K. The resulting g factors for the even-A isotopes (second column of Table II) have much smaller uncertainties than could be obtained in previous measurements. In Sec. III C, these new values are compared with the theory.

Spalding[7] extended the earlier work to include hfs measurements on the $^5I_{4,5}$ states of the odd-A isotopes ^{143,145}Nd. As a preliminary to our work on the higher metastable states, measurements of the $\Delta F=\pm 1$ transition frequencies were repeated. The results are consistent with Spalding's, but the uncertainty has been reduced an order of magnitude. From these data, accurate values for the dipole and quadrupole constants A and B could be obtained for the $^5I_{4,5}$ states by a computer program based on Eq. (1).

Approximate values for A and B in the $^5I_6$ state could then be predicted from the accurate results for the $^5I_{4,5}$ states and the theory of the J dependence of hfs constants outlined in Sec. III E. Computer predictions of the $^5I_6$, $\Delta F=0$ resonance frequencies, based on these rough calculated values

TABLE I. Relative population in individual magnetic substates of the low atomic levels of several Nd isotopes. The populations are normalized to 10 000 for each substate of the $^5I_4$ ground level of ^{142}Nd, the most abundant stable isotope.

Atomic state	Excitation energy (cm^{-1})	Relative population per atomic substate ^{142}Nd	^{143}Nd	^{145}Nd
$^5I_4$	0	10 000	561	382
$^5I_5$	1128	3 997	226	153
$^5I_6$	2367	1 461	83	56
$^5I_7$	3682	501	27	20
$^5I_8$	5049	166	10	7

of A and B and on the accurate g_J value observed in ^{142}Nd, soon led to observation of these transitions. Because of the strong undeflected beam of atoms with $m_J = 0$, however, it was difficult to observe the single-quantum flop-out $\Delta F = 0$, $\Delta M = 1$ transitions. Instead, a central obstacle was used to block most of the beam, and double-quantum transitions ($\nu = \Delta E/2h$) were induced. As the field was increased and the Zeeman spacings became less even, however, the double-quantum transitions were difficult to induce even with high rf power.

To solve this problem, the two-frequency technique of Prior *et al.*[18] was employed. In this procedure, the central obstacle is used as before to block the large undeflected portion of the beam, but the two single-quantum jumps required for an observable flop-in transition are induced successively by application of the *two* appropriate rf frequencies. Figure 1(a) shows such an observation in the $^5I_6$ state of ^{143}Nd at $H = 200$ G. For the observation, one rf generator supplied the fixed frequency 197.353 MHz, expected to be correct for the transition $(F, M \leftrightarrow F', M') = (\frac{19}{2}, \frac{9}{2} \leftrightarrow \frac{19}{2}, \frac{7}{2})$, while the second rf source was swept repeatedly through the range represented by the abscissa. Observation of the resonance was interpreted to indicate that atoms were successively undergoing the two single-quantum jumps $(\frac{19}{2}, \frac{9}{2} \leftrightarrow \frac{19}{2}, \frac{7}{2} \leftrightarrow \frac{19}{2}, \frac{5}{2})$, which correspond to the change $m_J = 1 \leftrightarrow 0 \leftrightarrow -1$ required for an observable flop-in effect. The roles of the two frequencies were then interchanged and the process repeated, as shown in Table III. Such observations were carried out for analogous transitions in the $^5I_6$ state of ^{143}Nd for $F = \frac{19}{2}, \frac{17}{2}, \frac{15}{2}$, and $\frac{13}{2}$, as indicated in Table IV which summarizes the observed transitions in ^{143}Nd.

A computer program then varied A and B to produce a best least-squares fit to the data with the aid of the accurately known value of g_J. The best fit to these data led to an unacceptable $\chi^2 = 583$, with a number of residuals exceeding 12 standard deviations. It was then found that if the computer were asked to fit only the *sum* of the fixed frequency and the frequency observed for resonance (rather than both separately), then all of the observations could be fitted very well ($\chi^2 = 10$). The conclusion was that we were observing two-quantum transitions rather than successive single-quantum transitions. Thus, the atom was interacting simultaneously with two unequal quanta such that $h\nu_\alpha + h\nu_\beta = \Delta E$, $\nu_\alpha \neq \nu_\beta$. The effect was then investigated in detail, using the ^{119}Sn atom in the $^3P_1$ state for convenience, and the results were published.[19] The dashed vertical line in Fig. 1(a) shows the resonance frequency calculated for the single-quantum transition $(\frac{19}{2}, \frac{7}{2} \leftrightarrow \frac{19}{2}, \frac{5}{2})$ from the precise A and B values later found from $\Delta F = \pm 1$ observations. It was subsequently found that if the rf level were increased enough, it was possible (even at 200 G) to observe the double-quantum ($\nu_\alpha = \nu_\beta$) transition $h\nu = \frac{1}{2}\Delta E$, as shown in Fig. 1(b). All of the relevant numbers are summarized in Table III. Other examples of both types of two-quantum observations are given in Table IV.

The same two-quantum ($\nu_\alpha \neq \nu_\beta$) technique was then applied to the $^5I_{4,5}$ states of ^{143}Nd to measure the g factors. As can be seen in Table II, the results are in excellent agreement with those deter-

TABLE II. Observed and calculated values of the electron g factor g_J for the members of the ^5I ground term. The values labeled "expt" are weighted averages of those obtained from the even-even isotopes and those from ^{143}Nd; the calculated values are for the Conway-Wybourne eigenvector description of the states.

Atomic state	Observed values of g_J Even-even	^{143}Nd	Expt.	Calculated g_J	$g_J^{\text{expt}} - g_J^{\text{calc}}$
$^5I_4$	0.603 30(3)	0.603 29(2)	0.603 29(2)	0.603 02	0.000 27
$^5I_5$	0.900 48(4)	0.900 47(3)	0.900 47(3)	0.900 41	0.000 06
$^5I_6$	1.069 93(5)	1.069 90(2)	1.069 91(2)	1.069 81	0.000 10
$^5I_7$	1.175 39(4)	1.175 37(2)	1.175 38(2)	1.175 13	0.000 25
$^5I_8$	1.245 21(5)	1.245 29(3)	1.245 27(3)	1.244 79	0.000 48

TABLE III. Summary of two-quantum observations of the $(\frac{19}{2}, \frac{9}{2} \longleftrightarrow \frac{19}{2}, \frac{5}{2})$ transition in the $^5I_6$ state of ^{143}Nd at 200 G. The transitions considered are listed in the first column, and the second gives the frequencies calculated for resonance from the final precise values of A, B, C, and g_J. The right-hand column gives at the bottom the resonance frequency observed for the usual double-quantum ($2h\nu = \Delta E$) method of inducing the transition, and columns 3 and 4 summarize observations in which two rf signals were simultaneously applied to the rf loop. In each case, the frequency in parentheses was held fixed, and a resonance appeared when the swept signal passed through the other listed value. It is seen that for runs 1 and 2, neither of the frequencies applied is consistent with the known energy intervals, but the sum of the two is. The transitions induced are of the type $h\nu_\alpha + h\nu_\beta = \Delta E$, $\nu_\alpha \neq \nu_\beta$.

Transition	Calculated resonance frequency (MHz)	Observed resonance frequency (MHz) Two-frequency technique Run No. 1	Two-frequency technique Run No. 2	Single-frequency double-quantum technique
$(\frac{19}{2}, \frac{9}{2} \longleftrightarrow \frac{19}{2}, \frac{7}{2})$	197.244(4)	(197.353)	197.345(20)	
$(\frac{19}{2}, \frac{7}{2} \longleftrightarrow \frac{19}{2}, \frac{5}{2})$	195.476(4)	195.355(12)	(195.400)	
Sum of above	392.720(6)	392.708(12)	392.745(20)	
One-half of sum	196.360(4)	196.354(9)	196.373(14)	196.367(7)

mined from the even-A isotopes for the states $^5I_{4,5,6}$.

Once the 200-G $\Delta F = 0$ data on the $^5I_6$ state of ^{143}Nd had been understood, the computer program led to values of A and B with sufficiently small uncertainty that the resonance frequencies for $\Delta F = \pm 1$ transitions could be closely predicted at low field. A number of these transitions were then observed, as indicated in Table IV. Several of the $\Delta F = \pm 1$ transitions listed for $^5I_{4,5,6}$ are of the flop-out type.

With accurate knowledge of the hfs constants for the three states $^5I_{4,5,6}$, the theory of the J dependence of hfs constants discussed in Sec. III E enables one to predict A and B for the $^5I_7$ state of ^{143}Nd with some precision. Several $\Delta F = 0$ transitions were then observed at 100 and 200 G. Figure 2 shows, for example, the appearance of the $(\frac{19}{2}, \frac{7}{2} \longleftrightarrow \frac{19}{2}, \frac{3}{2})$ transition in the $^5I_7$ state of ^{143}Nd at 200 G. This is a double-quantum single-frequency

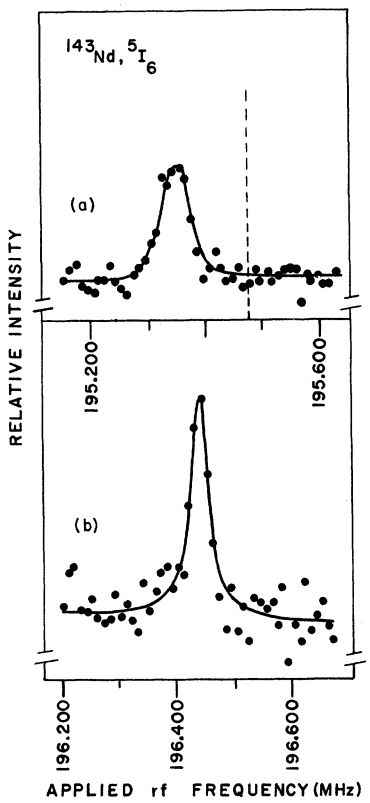

FIG. 1. Two-quantum observations of the $(\frac{19}{2}, \frac{9}{2} \longleftrightarrow \frac{19}{2}, \frac{5}{2})$ transition in the $^5I_6$ metastable atomic state of ^{143}Nd. (a) Spectrum obtained when two rf signals, one held fixed and one swept as shown, were simultaneously applied to the rf loop. The observed resonance requires both, and is of the type $h\nu_\alpha + h\nu_\beta = \Delta E$, $\nu_\alpha \neq \nu_\beta$. (b) Spectrum obtained when a single strong rf signal is applied. The resonance is of the type $2h\nu = \Delta E$.

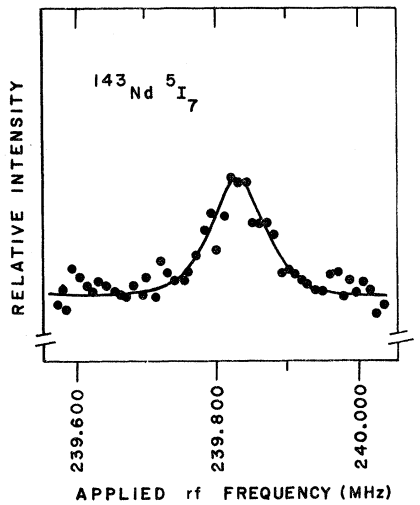

FIG. 2. Appearance of the $(\frac{19}{2}, \frac{7}{2} \longleftrightarrow \frac{19}{2}, \frac{3}{2})$ transition in the $^5I_7$ state of ^{143}Nd at $H = 200$ G. The time required to gather the data for the curve was ~20 min.

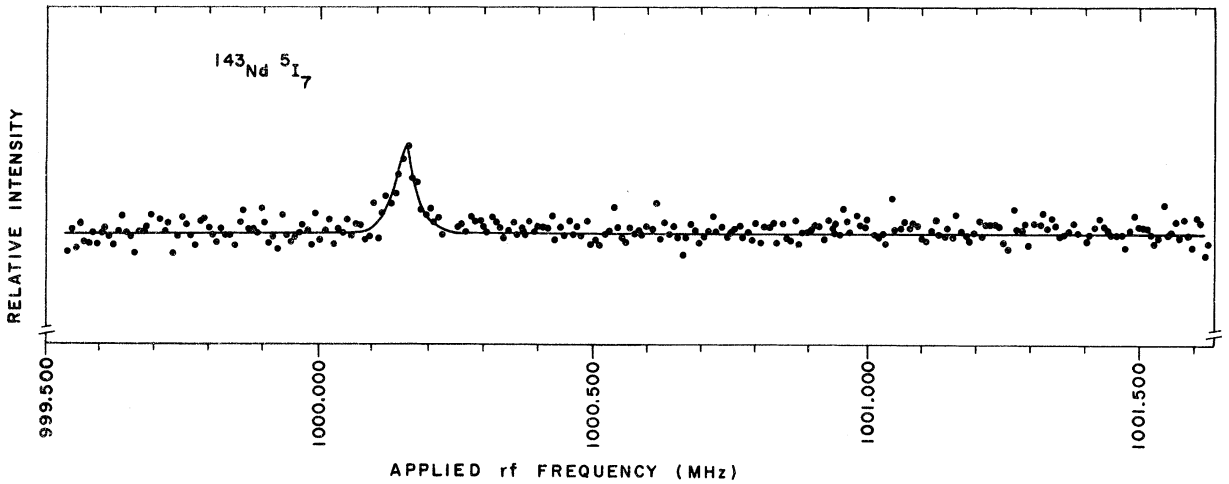

FIG. 3. Data from a wide sweep used to search for one Zeeman component of the $F=\frac{15}{2} \longleftrightarrow \frac{17}{2}$ interval in the $^5I_7$ state of ^{143}Nd at $H=1$ G. The zero-field interval is $\Delta\nu = 998.775$ MHz. Once the transition had been found, a much narrower sweep could be used to obtain better statistics over the resonance itself.

observation. Several observations of this type made possible accurate prediction of the resonance frequencies for $\Delta F = \pm 1$ transitions at 1 G. Figure 3 shows a wide sweep at 1 G made to find the $(\frac{15}{2}, \frac{3}{2} \leftrightarrow \frac{17}{2}, \frac{1}{2})$ transition in ^{143}Nd $^5I_7$. The procedure for the $^5I_8$ state was virtually identical to that described for $^5I_7$ except that the lower intensity made it much more difficult. Figure 4 shows a $\Delta F = \pm 1$ transition in the $^5I_8$ state of ^{143}Nd at 1 G. Higher-lying states in Nd could not be studied without major modification of technique.

The resonance frequency of each transition in ^{145}Nd can be accurately predicted from the hfs constants of the same state in ^{143}Nd once the ratios of the hfs constants for the two isotopes are established in the ground state, as was done by Spalding.[7] Because the abundance of ^{145}Nd is lower than that of ^{143}Nd, it was not possible to observe transitions in the $^5I_8$ state of the former. Table V lists all the observations in ^{145}Nd.

In Table VI, the columns labeled "uncorrected" give the values found for the hfs constants A, B, and C from the least-squares computer fits to the data of Tables IV and V. These fits were based on Eq. (1). The corrections applied to obtain the final values will be discussed in Sec. III F.

III. THEORETICAL CONSIDERATIONS AND INTERPRETATION OF RESULTS

A. Introduction

The position taken in this section is that the observable properties of the ^5I states should be consistent with the eigenvectors for the states if the appropriate radial integrals are regarded as adjustable parameters. The hfs integrals are overdetermined, and sensitive self-consistency tests are possible. The eigenvectors, which were deduced from fits to the excitation energies of the states, will thus be severely tested by investigating the degree to which they are consistent with the precise hyperfine and Zeeman results. Finally, the empirical values found for the radial integrals will be compared with the values recently calculated by the relativistic Hartree-Fock-Slater technique.

B. Eigenvectors

To obtain eigenvectors for the ^5I states, the complete matrix of the Coulomb and spin-orbit interactions is set up for all states of the $4f^46s^2$ con-

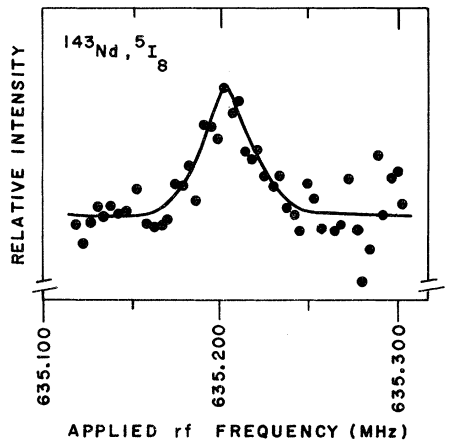

FIG. 4. Appearance of the $(\frac{9}{2}, -\frac{5}{2} \longleftrightarrow \frac{11}{2}, -\frac{7}{2})$ transition in the $^5I_8$ metastable state of ^{143}Nd at $H=1$ G. This observation required about 2 h of repeated sweeping, and is near the present limit of sensitivity. It was not possible to see the corresponding transition in ^{145}Nd with confidence.

figuration. The matrix elements are linear combinations of Slater integrals F_k and the spin-orbit constant ζ_{4f}. Since only the five levels $^5I_{4,5,6,7,8}$ had been identified experimentally, it was necessary to limit the number of radial integrals treated as adjustable parameters. Judd and Lindgren,[5] and later Conway and Wybourne,[6] did this by assuming that the Slater ratios F_4/F_2 and F_6/F_2 were hydrogenic. They thereby reduced the number of parameters to two: F_2 and ζ_{4f}. The matrices were then diagonalized, and the lowest five eigenvalues were fitted to the ^5I energies by varying F_2 and ζ_{4f} in the matrix elements. Although Conway and Wybourne found it possible to fit these levels to a mean error of only 2 cm^{-1}, they pointed out that lack of knowledge of all higher levels in

TABLE IV. Summary of observations in ^{143}Nd. Most of the transitions observed are single-quantum jumps. For those transitions that were observed by ordinary double-quantum jumps, the actual frequency $\nu = \Delta E/2h$ observed for resonance is given. For the two-frequency observations (marked with an asterisk in the table) in which $h\nu_\alpha + h\nu_\beta = \Delta E$, $\nu_\alpha \neq \nu_\beta$, the individual frequencies ν_α and ν_β are meaningless and the sum of the two is given instead.

Atomic state	Transition $(F, M \longleftrightarrow F', M')$	H (G)	Observed resonance frequency (MHz)	$\nu^{obs} - \nu^{calc}$ (kHz)
$^5I_4$	$(\frac{15}{2}, \frac{9}{2} \longleftrightarrow \frac{15}{2}, \frac{5}{2})$	200.000(5)	92.606(5)	−2
	$(\frac{15}{2}, \frac{3}{2} \longleftrightarrow \frac{15}{2}, \frac{5}{2})$	200.000(5)	185.221(13)*	5
	$(\frac{9}{2}, \frac{3}{2} \longleftrightarrow \frac{9}{2}, -\frac{1}{2})$	200.000(5)	205.012(14)*	1
	$(\frac{13}{2}, \frac{7}{2} \longleftrightarrow \frac{15}{2}, \frac{5}{2})$	1.000(5)	1418.603(10)	−3
	$(\frac{11}{2}, \frac{5}{2} \longleftrightarrow \frac{13}{2}, \frac{3}{2})$	1.000(5)	1258.012(10)	10
	$(\frac{9}{2}, \frac{3}{2} \longleftrightarrow \frac{11}{2}, \frac{1}{2})$	1.000(5)	1085.194(5)	−2
	$(\frac{7}{2}, \frac{1}{2} \longleftrightarrow \frac{9}{2}, -\frac{1}{2})$	1.000(5)	902.056(7)	−6
	$(\frac{5}{2}, -\frac{1}{2} \longleftrightarrow \frac{7}{2}, -\frac{3}{2})$	1.000(5)	710.450(9)	1
	$(\frac{5}{2}, -\frac{3}{2} \longleftrightarrow \frac{7}{2}, -\frac{5}{2})$	1.000(5)	710.362(9)	4
	$(\frac{5}{2}, -\frac{5}{2} \longleftrightarrow \frac{7}{2}, -\frac{7}{2})$	1.000(5)	710.272(9)	4
$^5I_5$	$(\frac{3}{2}, \frac{1}{2} \longleftrightarrow \frac{9}{2}, -\frac{3}{2})$	200.000(5)	407.647(13)*	0
	$(\frac{3}{2}, \frac{1}{2} \longleftrightarrow \frac{9}{2}, \frac{3}{2})$	200.000(5)	407.650(18)*	3
	$(\frac{3}{2}, \frac{1}{2} \longleftrightarrow \frac{9}{2}, \frac{3}{2})$	200.000(5)	407.645(22)*	−2
	$(\frac{15}{2}, \frac{7}{2} \longleftrightarrow \frac{17}{2}, \frac{5}{2})$	1.000(5)	1264.956(9)	−2
	$(\frac{13}{2}, \frac{5}{2} \longleftrightarrow \frac{15}{2}, \frac{3}{2})$	1.000(5)	1138.324(9)	5
	$(\frac{11}{2}, \frac{3}{2} \longleftrightarrow \frac{13}{2}, \frac{1}{2})$	1.000(5)	1003.410(7)	−4
	$(\frac{7}{2}, \frac{1}{2} \longleftrightarrow \frac{11}{2}, -\frac{1}{2})$	1.000(5)	861.330(9)	0
	$(\frac{7}{2}, -\frac{1}{2} \longleftrightarrow \frac{9}{2}, -\frac{3}{2})$	1.000(5)	713.116(9)	2
	$(\frac{5}{2}, -\frac{5}{2} \longleftrightarrow \frac{7}{2}, -\frac{7}{2})$	1.000(5)	559.160(6)	0
	$(\frac{5}{2}, -\frac{3}{2} \longleftrightarrow \frac{7}{2}, -\frac{5}{2})$	1.000(5)	559.612(11)	−2
$^5I_6$	$(\frac{19}{2}, \frac{9}{2} \longleftrightarrow \frac{19}{2}, \frac{5}{2})$	10.000(5)	9.485(11)	9
	$(\frac{15}{2}, \frac{5}{2} \longleftrightarrow \frac{15}{2}, \frac{1}{2})$	10.000(5)	10.580(12)	−10
	$(\frac{19}{2}, \frac{9}{2} \longleftrightarrow \frac{19}{2}, \frac{5}{2})$	50.000(5)	47.705(12)	−18
	$(\frac{17}{2}, \frac{7}{2} \longleftrightarrow \frac{17}{2}, \frac{3}{2})$	50.000(5)	50.090(11)	−8
	$(\frac{15}{2}, \frac{5}{2} \longleftrightarrow \frac{15}{2}, \frac{1}{2})$	50.000(5)	53.360(15)	6
	$(\frac{13}{2}, \frac{3}{2} \longleftrightarrow \frac{13}{2}, -\frac{1}{2})$	50.000(5)	57.945(15)	−21
	$(\frac{11}{2}, \frac{1}{2} \longleftrightarrow \frac{11}{2}, -\frac{3}{2})$	50.000(5)	64.760(10)	−11
	$(\frac{17}{2}, \frac{7}{2} \longleftrightarrow \frac{17}{2}, \frac{5}{2})$	100.000(5)	101.585(20)	−5
	$(\frac{15}{2}, \frac{5}{2} \longleftrightarrow \frac{15}{2}, \frac{3}{2})$	100.000(5)	108.445(20)	0
	$(\frac{13}{2}, \frac{3}{2} \longleftrightarrow \frac{13}{2}, \frac{1}{2})$	100.000(5)	118.085(20)	−1
$^5I_6$	$(\frac{11}{2}, \frac{1}{2} \longleftrightarrow \frac{11}{2}, -\frac{1}{2})$	100.000(5)	132.290(16)	25
	$(\frac{9}{2}, -\frac{1}{2} \longleftrightarrow \frac{9}{2}, -\frac{3}{2})$	100.000(5)	154.810(16)	−21
	$(\frac{19}{2}, \frac{9}{2} \longleftrightarrow \frac{19}{2}, \frac{5}{2})$	200.000(5)	392.714(20)*	0
	$(\frac{19}{2}, \frac{9}{2} \longleftrightarrow \frac{19}{2}, \frac{5}{2})$	200.000(5)	196.367(7)	10
	$(\frac{17}{2}, \frac{7}{2} \longleftrightarrow \frac{17}{2}, \frac{3}{2})$	200.000(5)	414.010(30)*	−46
	$(\frac{17}{2}, \frac{7}{2} \longleftrightarrow \frac{17}{2}, \frac{3}{2})$	200.000(5)	207.044(7)	16
	$(\frac{15}{2}, \frac{5}{2} \longleftrightarrow \frac{15}{2}, \frac{1}{2})$	200.000(5)	442.908(30)*	9
	$(\frac{15}{2}, \frac{5}{2} \longleftrightarrow \frac{15}{2}, \frac{1}{2})$	200.000(5)	221.445(7)	−5
	$(\frac{13}{2}, \frac{3}{2} \longleftrightarrow \frac{13}{2}, -\frac{1}{2})$	200.000(5)	483.397(50)*	−4
	$(\frac{13}{2}, \frac{3}{2} \longleftrightarrow \frac{13}{2}, -\frac{1}{2})$	200.000(5)	241.690(7)	−10

TABLE IV. (*Continued*)

Atomic state	Transition $(F, M \longleftrightarrow F', M')$	H (G)	Observed resonance frequency (MHz)	$\nu^{obs} - \nu^{calc}$ (kHz)
	$(\frac{5}{2}, -\frac{5}{2} \longleftrightarrow \frac{7}{2}, -\frac{7}{2})$	1.000(5)	476.973(7)	−1
	$(\frac{7}{2}, -\frac{3}{2} \longleftrightarrow \frac{9}{2}, -\frac{5}{2})$	1.000(5)	610.115(9)	7
	$(\frac{7}{2}, -\frac{3}{2} \longleftrightarrow \frac{9}{2}, \frac{5}{2})$	1.000(5)	610.105(14)	−3
	$(\frac{9}{2}, -\frac{1}{2} \longleftrightarrow \frac{11}{2}, -\frac{3}{2})$	1.000(5)	738.706(7)	−1
	$(\frac{11}{2}, \frac{1}{2} \longleftrightarrow \frac{13}{2}, -\frac{1}{2})$	1.000(5)	862.768(12)	−13
	$(\frac{13}{2}, \frac{3}{2} \longleftrightarrow \frac{15}{2}, \frac{1}{2})$	1.000(5)	981.754(12)	7
	$(\frac{15}{2}, \frac{5}{2} \longleftrightarrow \frac{17}{2}, \frac{3}{2})$	1.000(5)	1094.887(8)	1
	$(\frac{17}{2}, \frac{7}{2} \longleftrightarrow \frac{19}{2}, \frac{5}{2})$	1.000(5)	1201.440(13)	−2
$^5I_7$	$(\frac{21}{2}, \frac{9}{2} \longleftrightarrow \frac{21}{2}, \frac{5}{2})$	200.000(5)	227.125(15)	−3
	$(\frac{19}{2}, \frac{7}{2} \longleftrightarrow \frac{19}{2}, \frac{3}{2})$	200.000(5)	239.830(17)	−8
	$(\frac{17}{2}, \frac{5}{2} \longleftrightarrow \frac{17}{2}, \frac{1}{2})$	200.000(5)	256.645(15)	10
	$(\frac{15}{2}, \frac{3}{2} \longleftrightarrow \frac{15}{2}, -\frac{1}{2})$	200.000(5)	279.692(8)	7
	$(\frac{13}{2}, \frac{1}{2} \longleftrightarrow \frac{13}{2}, -\frac{3}{2})$	200.000(5)	313.415(9)	−9
	$(\frac{11}{2}, -\frac{1}{2} \longleftrightarrow \frac{11}{2}, -\frac{5}{2})$	200.000(5)	369.135(15)	1
	$(\frac{19}{2}, \frac{7}{2} \longleftrightarrow \frac{21}{2}, \frac{5}{2})$	1.000(5)	1194.580(8)	−3
	$(\frac{17}{2}, \frac{5}{2} \longleftrightarrow \frac{19}{2}, \frac{3}{2})$	1.000(5)	1100.280(5)	6
	$(\frac{15}{2}, \frac{3}{2} \longleftrightarrow \frac{17}{2}, \frac{1}{2})$	1.000(5)	1000.168(9)	−4
	$(\frac{13}{2}, \frac{1}{2} \longleftrightarrow \frac{15}{2}, -\frac{1}{2})$	1.000(5)	894.862(16)	−9
	$(\frac{11}{2}, -\frac{1}{2} \longleftrightarrow \frac{13}{2}, -\frac{3}{2})$	1.000(5)	784.930(10)	−4
	$(\frac{9}{2}, -\frac{3}{2} \longleftrightarrow \frac{11}{2}, -\frac{5}{2})$	1.000(5)	670.840(6)	3
	$(\frac{7}{2}, -\frac{5}{2} \longleftrightarrow \frac{9}{2}, -\frac{7}{2})$	1.000(5)	552.760(25)	1
$^5I_8$	$(\frac{17}{2}, \frac{3}{2} \longleftrightarrow \frac{17}{2}, -\frac{1}{2})$	200.000(5)	305.642(16)	11
	$(\frac{21}{2}, \frac{7}{2} \longleftrightarrow \frac{21}{2}, \frac{3}{2})$	200.000(5)	263.925(30)	−3
	$(\frac{13}{2}, -\frac{1}{2} \longleftrightarrow \frac{13}{2}, -\frac{5}{2})$	200.000(5)	389.635(13)	−11
	$(\frac{15}{2}, \frac{1}{2} \longleftrightarrow \frac{15}{2}, -\frac{3}{2})$	200.000(5)	339.050(13)	−7
	$(\frac{19}{2}, \frac{5}{2} \longleftrightarrow \frac{19}{2}, \frac{1}{2})$	200.000(5)	281.795(30)	4
	$(\frac{23}{2}, \frac{9}{2} \longleftrightarrow \frac{23}{2}, \frac{5}{2})$	200.000(5)	250.090(15)	−18
	$(\frac{9}{2}, -\frac{5}{2} \longleftrightarrow \frac{11}{2}, -\frac{7}{2})$	1.000(5)	635.202(8)	0
	$(\frac{9}{2}, -\frac{5}{2} \longleftrightarrow \frac{11}{2}, -\frac{7}{2})$	1.006(5)	635.210(10)	4
	$(\frac{11}{2}, -\frac{3}{2} \longleftrightarrow \frac{13}{2}, -\frac{5}{2})$	1.000(5)	744.475(20)	−9
	$(\frac{11}{2}, -\frac{3}{2} \longleftrightarrow \frac{13}{2}, -\frac{5}{2})$	1.000(5)	744.480(20)	−4
	$(\frac{13}{2}, -\frac{1}{2} \longleftrightarrow \frac{15}{2}, -\frac{3}{2})$	1.000(5)	850.003(15)	−8
	$(\frac{13}{2}, -\frac{1}{2} \longleftrightarrow \frac{15}{2}, -\frac{3}{2})$	1.000(5)	850.025(25)	14
	$(\frac{15}{2}, \frac{1}{2} \longleftrightarrow \frac{17}{2}, -\frac{1}{2})$	1.000(5)	951.500(25)	−27
	$(\frac{15}{2}, \frac{1}{2} \longleftrightarrow \frac{17}{2}, -\frac{1}{2})$	1.000(5)	951.550(20)	23

TABLE V. Summary of observations in ^{145}Nd. All observations are of single-quantum $\Delta F = \pm 1$ transitions, and all were made at $H = 1$ G.

Atomic state	Transition $(F, M \leftrightarrow F', M')$	H (G)	Observed resonance frequency (MHz)	$\nu^{obs} - \nu^{calc}$ (kHz)
$^5I_4$	$(\frac{13}{2}, \frac{7}{2} \leftrightarrow \frac{15}{2}, \frac{5}{2})$	1.000(5)	886.718(7)	−1
	$(\frac{11}{2}, \frac{5}{2} \leftrightarrow \frac{13}{2}, \frac{3}{2})$	1.000(5)	783.574(9)	0
	$(\frac{9}{2}, \frac{3}{2} \leftrightarrow \frac{11}{2}, \frac{1}{2})$	1.000(5)	674.000(10)	4
	$(\frac{7}{2}, \frac{1}{2} \leftrightarrow \frac{9}{2}, -\frac{1}{2})$	1.000(5)	558.976(6)	4
	$(\frac{5}{2}, -\frac{5}{2} \leftrightarrow \frac{7}{2}, -\frac{7}{2})$	1.000(5)	439.282(8)	1
	$(\frac{5}{2}, -\frac{3}{2} \leftrightarrow \frac{7}{2}, -\frac{5}{2})$	1.000(5)	439.365(8)	−5
	$(\frac{5}{2}, -\frac{1}{2} \leftrightarrow \frac{7}{2}, -\frac{3}{2})$	1.000(5)	439.452(9)	−8
$^5I_5$	$(\frac{15}{2}, \frac{7}{2} \leftrightarrow \frac{17}{2}, \frac{5}{2})$	1.000(5)	790.653(9)	−4
	$(\frac{13}{2}, \frac{5}{2} \leftrightarrow \frac{15}{2}, \frac{3}{2})$	1.000(5)	709.403(9)	2
	$(\frac{11}{2}, \frac{3}{2} \leftrightarrow \frac{13}{2}, \frac{1}{2})$	1.000(5)	623.788(9)	4
	$(\frac{9}{2}, \frac{1}{2} \leftrightarrow \frac{11}{2}, -\frac{1}{2})$	1.000(5)	534.380(9)	5
	$(\frac{7}{2}, -\frac{1}{2} \leftrightarrow \frac{9}{2}, -\frac{3}{2})$	1.000(5)	441.694(8)	−3
	$(\frac{5}{2}, -\frac{3}{2} \leftrightarrow \frac{7}{2}, -\frac{5}{2})$	1.000(5)	346.075(9)	−5
$^5I_6$	$(\frac{5}{2}, -\frac{5}{2} \leftrightarrow \frac{7}{2}, -\frac{7}{2})$	1.000(5)	294.405(25)	3
	$(\frac{7}{2}, -\frac{3}{2} \leftrightarrow \frac{9}{2}, -\frac{5}{2})$	1.000(5)	377.568(12)	−6
	$(\frac{9}{2}, -\frac{1}{2} \leftrightarrow \frac{11}{2}, -\frac{3}{2})$	1.000(5)	457.845(10)	−15
	$(\frac{11}{2}, \frac{1}{2} \leftrightarrow \frac{13}{2}, -\frac{1}{2})$	1.000(5)	535.666(9)	29
	$(\frac{13}{2}, \frac{3}{2} \leftrightarrow \frac{15}{2}, \frac{1}{2})$	1.000(5)	610.673(12)	−7
	$(\frac{15}{2}, \frac{5}{2} \leftrightarrow \frac{17}{2}, \frac{3}{2})$	1.000(5)	682.620(9)	−14
	$(\frac{17}{2}, \frac{7}{2} \leftrightarrow \frac{19}{2}, \frac{5}{2})$	1.000(5)	751.110(13)	10
$^5I_7$	$(\frac{19}{2}, \frac{7}{2} \leftrightarrow \frac{21}{2}, \frac{5}{2})$	1.000(5)	747.027(20)	0
	$(\frac{17}{2}, \frac{5}{2} \leftrightarrow \frac{19}{2}, \frac{3}{2})$	1.000(5)	686.222(15)	2
	$(\frac{15}{2}, \frac{3}{2} \leftrightarrow \frac{17}{2}, \frac{1}{2})$	1.000(5)	622.352(12)	−8
	$(\frac{13}{2}, \frac{1}{2} \leftrightarrow \frac{15}{2}, -\frac{1}{2})$	1.000(5)	555.768(14)	16
	$(\frac{11}{2}, -\frac{1}{2} \leftrightarrow \frac{13}{2}, -\frac{3}{2})$	1.000(5)	486.668(11)	0
	$(\frac{9}{2}, -\frac{3}{2} \leftrightarrow \frac{11}{2}, -\frac{5}{2})$	1.000(5)	415.286(11)	−11
	$(\frac{7}{2}, -\frac{5}{2} \leftrightarrow \frac{9}{2}, -\frac{7}{2})$	1.000(5)	341.540(17)	13

$4f^4 6s^2$, and neglect of configuration interaction and the smaller magnetic interactions, could lead to deficiencies in the eigenvectors even though the energy fit appeared excellent. The eigenvectors listed in Table VII are those found by Conway and Wybourne,[6] except that several errors subsequently found by Conway[20] have been corrected. One notices immediately that even the least-pure state, namely $^5I_8$, is 96.4% pure. The largest impurity in any ^5I state, namely, the $^3K(2)$ component of $^5I_8$, is 2.8%. (The parenthetic numbers in the designations of this and other impurities listed in the first column of Table VII refer to the convention Nielson and Koster[21] established to distinguish between LS basis states of the same S and L.) Because of the high LS purity of the ^5I states, it is convenient to retain the designation ^5I, while recognizing that there are small admixtures of states of different S and L present. Although the eigenvectors (and all calculations in this paper) are in the SL scheme, the conventional phrases LS coupling, LS scheme, LS basis, etc., will be used.

C. Values of g_J

Because the Zeeman interaction has no radial dependence, g_J values can easily be calculated for all the basis states, and the g_J values in intermediate coupling follow immediately for states with specified eigenvectors. The calculation is particularly simple in the LS scheme because the cross terms all vanish. The next-to-last column of Table II lists the g_J values calculated in this way for the states represented by the Conway-Wybourne[6,20] eigenvectors of Table VII, after small corrections for relativistic and diamagnetic effects have been made. The corrections were made by Conway and Wybourne[6] for the states $^5I_{4,5,6}$ and were taken from Judd and Lindgren[5] for the other two states. The final column of Table II gives the difference between the calculated and observed values (the experimental value is a weighted average of that observed in the even-A Nd isotopes and that found from ^{143}Nd). The differences, though well outside experimental error, are remarkably small in absolute terms. The differences probably arise from approximations made in deriving the eigenvectors, as discussed in Sec. III B.

Judd and Lindgren[5] have given an expression which should be obeyed by the g_J values of the states of an LS multiplet. It takes account of the Schwinger, relativistic, diamagnetic, and second-order spin-orbit corrections to the g factor. Although it ignores the effects of configuration interaction, they are of higher order because the Coulomb interaction is diagonal in S, L, and J. The relation is

$$(J+1)g_J - (J-1)g_{J-1} = aJ^2 + b \ , \tag{5}$$

where for our purpose a and b may be regarded as empirical quantities. Thus, if they are evaluated by writing Eq. (5) with each of the experimental g_J values of the $^5I_{4,5,6}$ states and solving simultaneously, then Eq. (5) may be used to predict the g_J values of the remaining two states $^5I_{7,8}$. The predicted values are 1.175 42(18) and 1.245 33(20) for the states $^5I_7$ and $^5I_8$, respectively. These predictions are in good agreement with the measured values, as may be seen from Table II.

D. hfs Hamiltonian

The hyperfine Hamiltonian specified by Eqs. (1)–(4), while consistent with all of the present data, says nothing about the hfs constants A, B, and C, and in fact is unconcerned with any property of the atomic state but its total angular momen-

TABLE VI. Uncorrected and final values of the hfs constants A, B, and C for ^{143,145}Nd. The uncorrected values are those required to fit the observations by use of the Hamiltonian of Eqs. (1)–(4) in which J is assumed to be a good quantum number. The final values include small corrections for hyperfine interactions between ^5I states of different J. The corrections are smaller than experimental uncertainty in each case.

Atomic state	Quantity	Value of hyperfine constant (MHz) ^{143}Nd Uncorrected	^{143}Nd Final	^{145}Nd Uncorrected	^{145}Nd Final
$^5I_4$	A	−195.652(1)	−195.652(1)	−121.628(1)	−121.628(1)
	B	122.608(17)	122.595(17)	64.637(14)	64.632(14)
	C	0.001(2)	0.001(2)	0.001(2)	0.001(2)
$^5I_5$	A	−153.679(1)	−153.679(1)	−95.535(1)	−95.535(1)
	B	115.741(18)	115.743(18)	61.044(21)	61.045(21)
	C	0.000(2)	0.000(2)	0.001(2)	0.000(2)
$^5I_6$	A	−130.611(1)	−130.611(1)	−81.195(1)	−81.195(1)
	B	119.284(23)	119.291(23)	62.926(29)	62.929(29)
	C	−0.001(3)	−0.001(3)	0.004(4)	0.004(4)
$^5I_7$	A	−117.604(1)	−117.604(1)	−73.108(1)	−73.108(1)
	B	129.281(24)	129.291(24)	68.165(37)	68.168(37)
	C	0.002(3)	0.002(3)	−0.001(4)	−0.001(4)
$^5I_8$	A	−110.476(3)	−110.476(3)		
	B	143.937(87)	143.952(87)		

tum J. Thus while Eqs. (1)–(4) are suitable for extracting experimental values for hfs constants and g values from the observations, a more fundamental approach is required to interpret the values found for these constants.

The Hamiltonian for the hyperfine interaction may be written[22] as the sum of scalar products of suitable tensor operators, as

$$\mathcal{H}_{\rm hfs}=\sum_k \vec{\mathrm{T}}_e^{(k)}\cdot\vec{\mathrm{T}}_n^{(k)} , \tag{6}$$

where the subscripts e and n refer to the electrons and to the nucleus, respectively. The first three terms are the only ones of importance; they are the magnetic-dipole ($k=1$), the electric-quadrupole ($k=2$), and the magnetic-octupole ($k=3$). Of these, the first two are comparable in importance for ^{143,145}Nd and the third is found to be negligible.

Sandars and Beck[23] have shown that for a given k, the electronic factor $\vec{\mathrm{T}}_e^{(k)}$ in Eq. (6) can consist of at most three terms for an atom with a single unfilled electron shell nl^N. These parts may be written as proportional to double tensor operators, introduced by Judd,[24] of the form $\vec{\mathrm{U}}^{(k_s,k_l)k}$, where k_s is the rank of the operator in spin space, k_l that in orbital space, and k that in the $\vec{\mathrm{J}}=\vec{\mathrm{s}}+\vec{\mathrm{l}}$ space. The three possible contributions to $\vec{\mathrm{T}}_e^{(k)}$ are $\vec{\mathrm{U}}^{(0,k)k}$, $\vec{\mathrm{U}}^{(1,k-1)k}$, and $\vec{\mathrm{U}}^{(1,k+1)k}$. For the dipole case, these are proportional to $\vec{\mathrm{L}}$, $\vec{\mathrm{S}}$, and $(\vec{\mathrm{s}}\,\vec{\mathrm{C}}^{(2)})^{(1)}$, respectively, and the effective-dipole hfs Hamiltonian may be written

$$\mathcal{H}_{\rm hfs}(M1)=\sum_{i=1}^{N}[\,a^{01}\vec{\mathrm{l}}_i-(10)^{1/2}(\vec{\mathrm{s}}\,\vec{\mathrm{C}}^{(2)})_i^{(1)}a^{12}+a^{10}\vec{\mathrm{s}}_i\,]\cdot\vec{\mathrm{I}} , \tag{7}$$

where the $a^{k_s k_l}$ are quantities which include electronic radial properties and are proportional to the nuclear g factor g_I. Sandars and Beck[23] also showed that if distortions of the $a^{k_s k_l}$ by configuration interaction are ignored, the radial quantities are given by

$$a^{01}=D(2l+1)^{-2}[\,2l(l+1)F_{++}+2l(l+1)F_{--}+F_{+-}\,] , \tag{8a}$$

$$a^{12}=\tfrac{1}{3}D(2l+1)^{-2}[\,-4l(l+1)(2l-1)F_{++}+4l(l+1)(2l+3)F_{--}-(2l+3)(2l-1)F_{+-}\,] , \tag{8b}$$

$$a^{10}=\tfrac{4}{3}Dl(l+1)(2l+1)^{-2}[\,(l+1)F_{++}-lF_{--}-F_{+-}\,] , \tag{8c}$$

where

$$D=(2\mu_B\mu_N/h)(\mu_I/I) , \tag{9}$$

the signs + and − refer to the cases $j=l+\frac{1}{2}$ and $j=l-\frac{1}{2}$, respectively, and μ_I is the nuclear dipole moment, measured in units of the nuclear magneton μ_N. The quantities $F_{jj'}$ are relativistic radial integrals given[23] by

$$F_{jj'}=-2\,[\alpha a_0(K+K'+2)]^{-1}\int_0^\infty (P_jQ_{j'}+Q_jP_{j'})r^{-2}\,dr , \tag{10}$$

where α is the fine-structure constant, a_0 is the Bohr radius, P_j and Q_j are the large and small components of the relativistic radial wave function, respectively, and K and K' are equal to $\pm(j+\frac{1}{2})$ for $l=j\pm\frac{1}{2}$. The $F_{jj'}$ have the nonrelativistic limit $\langle r^{-3}\rangle_{nl}$ and have recently been calculated[10,11] for Nd I by use of relativistic Hartree-Fock-Slater wave functions. The nuclear dipole moment μ_I, which occurs in Eq. (9), has been measured[8] in ^{143}Nd; the value is

TABLE VII. *SL* eigenvectors for the ^5I states of Nd I, as calculated by Conway and Wybourne. Several errors in Ref. 6 have been corrected by Conway in this table. In the list of basis states (column 1), the numbers in parentheses refer to Nielson and Koster's (Ref. 21) convention for distinguishing between *SL* states of the same *S* and *L*.

Basis state	$J=4$	$J=5$	$J=6$	$J=7$	$J=8$
^5I	0.9879	0.9932	0.9947	0.9910	0.9818
^5G	−0.0037	−0.0043	−0.0033		
^5F	0.0012	0.0012			
^5D	−0.0001				
^3M					0.0036
^3L				−0.0130	−0.0198
$^3K(1)$			−0.0323	−0.0585	−0.0830
$^3K(2)$			0.0607	0.1125	0.1683
$^3I(1)$		−0.0194	−0.0287	−0.0317	
$^3I(2)$		0.0175	0.0248	0.0257	
$^3H(1)$	0.0678	0.0484	0.0277		
$^3H(2)$	−0.0081	−0.0039			
$^3H(3)$	0.0777	0.0583	0.0350		
$^3H(4)$	−0.1138	−0.0835	−0.0492		
$^3G(1)$	0.0028	0.0016			
$^3G(2)$	0.0120	0.0088			
$^3G(3)$	−0.0074	−0.0052			
$^3F(1)$	−0.0006				
$^3F(2)$	0.0008				
$^3F(3)$	−0.0008				
$^3F(4)$	0.0016				
$^1L(1)$					0.0055
$^1L(2)$					0.0200
^1K				−0.0043	
$^1I(1)$			−0.0022		
$^1I(2)$			−0.0031		
$^1I(3)$			−0.0056		
$^1H(1)$		0.0036			
$^1H(2)$		0.0016			
$^1G(1)$	0.0071				
$^1G(2)$	−0.0035				
$^1G(3)$	0.0037				
$^1G(4)$	0.0112				

$$\mu_I(^{143}\mathrm{Nd}) = -1.063(5)\mu_N \ .$$

Thus, neglecting configuration interaction, one can use the experimental value of μ_I to evaluate a^{01}, a^{12}, and a^{10} theoretically for ^{143}Nd and can compare the resulting values with those determined experimentally. However, configuration interaction can be expected to play a non-negligible role.

The electric-quadrupole equivalent of Eq. (7) can be written in several ways, one of which[25] is

$$\mathcal{H}_{\mathrm{hfs}}(E2) = \frac{e^2 r_n^2}{r_e^3} \overleftrightarrow{C}_n^{(2)} \cdot \sum_{i=1}^{N} \left[\left(\frac{2l(l+1)(2l+1)}{(2l-1)(2l+3)} \right)^{1/2} \frac{b^{02}}{b_{nl}} \overleftrightarrow{U}_i^{(02)2} + \left(\frac{3}{10} \right)^{1/2} \frac{b^{13}}{b_{nl}} \overleftrightarrow{U}_i^{(13)2} + \left(\frac{3}{10} \right)^{1/2} \frac{b^{11}}{b_{nl}} \overleftrightarrow{U}_i^{(11)2} \right] , \quad (11)$$

where

$$e r_n^2 \overleftrightarrow{C}_n^{(2)} = \overleftrightarrow{T}_n^{(2)} \ , \quad (12)$$

$$\langle I, M_I = I | \, T_n^{(2)} \, | II \rangle = \tfrac{1}{2} eQ \ , \quad (13)$$

and

$$b_{nl} = e^2 Q \langle r^{-3} \rangle_{nl} \ , \quad (14)$$

where Q is the electric-quadrupole moment of the nucleus and $\langle r^{-3} \rangle_{nl}$ is the nonrelativistic expectation value of $1/r^3$ for the shell nl. In the nonrelativistic limit, the last two terms of Eq. (11) become zero, and b^{02} approaches the nonrelativistic parameter b_{nl}. In this limit, we note that the quadrupole interaction is entirely orbital in character ($k_s = 0$). The quantities $b^{k_s k_l}$ are analogous to the $a^{k_s k_l}$ of Eqs. (8); in the absence of configuration interaction, they are given[26] by

$$b^{02} = (e^2 Q/h)(2l+1)^{-2}[(l+2)(2l-1)R_{++} + (l-1)(2l+3)R_{--} + 6R_{+-}] \ , \quad (15a)$$

$$b^{13} = -\frac{2}{5} \frac{e^2 Q}{h} (2l+1)^{-1} \left(\frac{105(l+2)(l-1)l(l+1)}{(2l+3)(2l+1)(2l-1)} \right)^{1/2} \times [(2l-1)R_{++} - (2l+3)R_{--} + 4R_{+-}] \ , \quad (15b)$$

$$b^{11} = -\frac{2}{5} \frac{e^2 Q}{h} (2l+1)^{-1} \left(\frac{30l(l+1)}{2l+1} \right)^{1/2} \times [-(l+2)R_{++} + (l-1)R_{--} + 3R_{+-}] \ , \quad (15c)$$

in which the relativistic quadrupole radial integrals $R_{jj'}$ are defined[23] as

$$R_{jj'} = \int_0^\infty [P_j P_{j'} + Q_j Q_{j'}] r^{-3} dr \ . \quad (16)$$

The quantities b^{13} and b^{11} are entirely relativistic in origin, although configuration interaction may distort the values found for them empirically. The integrals $R_{jj'}$ have been calculated relativistically, as for the dipole equivalents $F_{jj'}$, but because there is no direct measurement of Q equivalent to that of μ_I, the values of $b^{k_s k_l}$ cannot be predicted as closely as can the $a^{k_s k_l}$.

The magnetic-octupole equivalent of Eqs. (7) and (11), which would be needed to predict the J dependence of the octupole hfs constants C, is not required since C was found to be zero to within experimental error for all five ^5I states.

E. Theoretical Values of A and B

If matrix elements of Eqs. (7) and (11) are taken between two *LS* basis states of the same J, it is found that

$$\langle l^N \alpha S L J I F M | \mathcal{H}_{\mathrm{hfs}}(M1) | l^N \alpha' S' L' J I F M \rangle = A(\psi, \psi') \langle J I F M | \vec{\mathrm{I}} \cdot \vec{\mathrm{J}} | J I F M \rangle \ , \quad (17)$$

$$\langle l^N \alpha S L J I F M | \mathcal{H}_{\mathrm{hfs}}(E2) | l^N \alpha' S' L' J I F M \rangle = B(\psi, \psi') Q_{\mathrm{op}} \ ,$$

where $\langle J I F M | \vec{\mathrm{I}} \cdot \vec{\mathrm{J}} | J I F M \rangle$ and Q_{op} are defined in Eqs. (4) and (2), respectively, and $A(\psi, \psi')$

$=A(\psi',\psi)$ and $B(\psi,\psi')=B(\psi',\psi)$ are generalized hfs constants between the indicated LS basis states.

Examination of the complete expressions[25] for the matrix elements shows that in Eqs. (17)

$$A(\psi,\psi')=(2-g_J^*)\delta(\alpha S L,\alpha' S' L')a^{01}+\left(\frac{30(2J+1)}{J(J+1)}\right)^{1/2}\left(\frac{l(l+1)(2l+1)}{(2l-1)(2l+3)}\right)^{1/2}$$
$$\times\langle l^N\alpha SL||V^{(12)}||l^N\alpha' S'L'\rangle\begin{Bmatrix}S & S' & 1\\ L & L' & 2\\ J & J & 1\end{Bmatrix}a^{12}+(g_J^*-1)\delta(\alpha SL,\alpha' S'L')a^{10}, \tag{18}$$

$$B(\psi,\psi')=\left(\frac{4J(2J+1)(2J-1)}{(J+1)(2J+3)}\right)^{1/2}\left[(-1)^{S+L'+J}\delta(S,S')\begin{Bmatrix}J & J & 2\\ L' & L & S\end{Bmatrix}\langle l^N\alpha SL||U^{(2)}||l^N\alpha' S'L'\rangle\left(\frac{l(l+1)(2l+1)}{(2l-1)(2l+3)}\right)^{1/2}b^{02}\right.$$
$$\left.+\begin{Bmatrix}S & S' & 1\\ L & L' & 3\\ J & J & 2\end{Bmatrix}\langle l^N\alpha SL||V^{(13)}||l^N\alpha' S'L'\rangle b^{13}+\begin{Bmatrix}S & S' & 1\\ L & L' & 1\\ J & J & 2\end{Bmatrix}\langle l^N\alpha SL||V^{(11)}||l^N\alpha' S'L'\rangle b^{11}\right],$$

where

$$g_J^*=1+[J(J+1)-L(L+1)+S(S+1)][2J(J+1)]^{-1} \tag{19}$$

is the Landé value of the g factor (without the Schwinger correction). The required reduced matrix elements of $U^{(2)}$ and $V^{(11)}$ have been tabulated by Nielson and Koster,[21] and those of $V^{(11)}$, $V^{(12)}$, and $V^{(13)}$ by Yutsis *et al.*[27] The 6-j symbols are given by Rotenberg *et al.*[28] and the required 9-j symbols can be evaluated from them.

With Eqs. (18) and the eigenvectors of Table VII, it is possible to obtain a linear three-parameter expression for each hfs A and B constant in the ^5I term. The results are

$$\begin{aligned}
A(^5I_4')&=1.395\,110a^{01}-0.012\,584a^{12}-0.395\,094a^{10},\\
A(^5I_5')&=1.098\,300a^{01}-0.007\,553a^{12}-0.098\,307a^{10},\\
A(^5I_6')&=0.929\,232a^{01}+0.001\,445a^{12}+0.070\,767a^{10},\\
A(^5I_7')&=0.824\,127a^{01}+0.016\,844a^{12}+0.175\,873a^{10},\\
A(^5I_8')&=0.754\,607a^{01}+0.037\,751a^{12}+0.245\,393a^{10},
\end{aligned} \tag{20}$$

$$\begin{aligned}
B(^5I_4')&=-0.219\,874b^{02}-0.070\,198b^{13}-0.120\,488b^{11},\\
B(^5I_5')&=-0.205\,018b^{02}-0.056\,402b^{13}-0.004\,426b^{11},\\
B(^5I_6')&=-0.209\,679b^{02}-0.034\,566b^{13}+0.095\,291b^{11},\\
B(^5I_7')&=-0.226\,221b^{02}-0.000\,865b^{13}+0.187\,251b^{11},\\
B(^5I_8')&=-0.253\,605b^{02}+0.044\,140b^{13}+0.275\,257b^{11}.
\end{aligned} \tag{21}$$

These expressions are for the complete eigenvectors of Conway and Wybourne[6,20] (Table VII); they have not been truncated.

F. Corrections for Off-Diagonal hfs

Before the parametrized expressions just developed for A and B can be fitted to the observed values, the resonance frequencies must be corrected for the perturbations caused by hyperfine and Zeeman interactions between ^5I states with *different* J. These corrections result in changes which are in each case less than experimental uncertainty. For this reason, the details will be omitted; the procedure for making the corrections is given, for example, by Woodgate.[29] The corrected values of the hfs constants are given in the right-hand column of Table VI. No corrections to the g values were required.

G. Isotopic Ratios of Hyperfine Constants, and the Hyperfine Anomaly

Once the corrected values of A and B have been determined for each state in the isotopes ^{143,145}Nd, ratios of corresponding hfs constants for the two isotopes can be evaluated. These are exhibited in Table VIII. Because no resonances were observed in the $^5I_8$ state of ^{145}Nd, the ratios can be given only for the four states $^5I_{4,5,6,7}$. The self-consistency of the results is good. From the entries in the table, the average values are found to be

$$A^{143}/A^{145}=1.608\,61(2), \tag{22}$$

$$B^{143}/B^{145}=1.896\,4(4). \tag{23}$$

These results are consistent with those of Spalding,[7] but have an uncertainty about 20 times smaller. They are not consistent with the dipole ratio 1.608 92(10) obtained by Erickson[30] by electron-paramagnetic-resonance absorption by trivalent Nd ions in monocrystals of $LaCl_3$ at zero magnetic field. The free atom is a much simpler system, and the values in Eqs. (22) and (23) should be freer of interpretational problems.

The nuclear dipole moments of the two isotopes have not been measured with comparable precision, and consequently a precise value of the hyperfine anomaly cannot be given. The most ac-

curate moment ratio available is

$$\mu_I(^{143}\mathrm{Nd})/\mu_I(^{145}\mathrm{Nd}) = 1.626(12)\,, \tag{24}$$

which is obtained from Table III of Smith and Unsworth.[8] While this appears larger than the ratio of the hyperfine constants in Eq. (22), the nuclear moments were measured at strong magnetic field, and further correction for off-diagonal hyperfine and Zeeman interactions within the ^5I term may be required. A direct measurement of the moment ratio would be very valuable.

The difference between the ratio of the A factors and that of the nuclear dipole moments gives the hyperfine anomaly immediately, and the anomaly indicated by Eqs. (22) and (24) is relatively very large, about 1%. However, it is doubtful if the anomaly actually is this large. Any anomaly would have to originate in the contact part of the hfs, and it is shown in Sec. III J that most of the contribution to this is probably from the relativistic term. While this term acts like a contact interaction, it is associated with $4f$ electrons and does not lead to an anomaly.[23] The extent of any true contact interaction, such as core polarization, is indistinguishable experimentally from the relativistic part and can be inferred only to the extent to which one can calculate the latter effect.

The ratio of the electric-quadrupole moments of the two isotopes should be the same as the B ratio (23); any difference should be extremely small.

H. Algebraic Signs of Hyperfine Constants

Smith and Unsworth[8] have shown that the algebraic sign of the dipole hfs constant A is negative for the $^5I_4$ atomic state in both ^{143}Nd and ^{145}Nd. The signs of the nuclear magnetic-dipole moments of ^{143}Nd and ^{145}Nd are both known[8] to be negative. With this information, it is easy to establish that the sign of A must be negative for all five ^5I atomic states in both isotopes. In Eqs. (20), for example, the orbital term (that involving a^{01}) is much larger than either of the other two. In the nonrelativistic limit where $F_{++} = F_{--} = F_{+-} = \langle r^{-3}\rangle_{4f}$, it can be seen by putting $l = 3$ in the first of Eqs. (8) that a^{01} becomes

$$a_{nl} = (2\mu_B\mu_N/\hbar)(\mu_I/I)\langle r^{-3}\rangle_{nl} \tag{25}$$

and that a^{01} and therefore A both have the same sign (negative) as μ_I. In the same limit, a^{12} also approaches a_{nl} and a^{10} approaches zero. (It should be remembered that configuration interaction can distort the values actually observed to some extent.) The algebraic sign of B/A is measured experimentally, and that of B therefore follows immediately.

TABLE VIII. Ratios of the dipole and quadrupole hfs constants of the isotopes ^{143}Nd and ^{145}Nd. It can be seen that, within experimental uncertainty, the ratios are independent of which atomic state is used for the measurement.

Atomic state	A^{143}/A^{145}	B^{143}/B^{145}
$^5I_4$	1.608 61 (2)	1.8968 (5)
$^5I_5$	1.608 61 (2)	1.8960 (7)
$^5I_6$	1.608 61 (2)	1.8956 (9)
$^5I_7$	1.608 63 (3)	1.8967 (11)

J. Values of Hyperfine Radial Parameters

Equations (20) and (21) give three-parameter expressions for the A and B values of the ^5I states for any particular Nd isotope. The parameters for ^{143}Nd, for example, are thus overdetermined by requiring the expressions to be consistent with the observed hfs constants of all five A's and B's in ^{143}Nd. The corresponding results for ^{145}Nd can then be obtained from the ratios of Eqs. (22) and (23). The three-parameter fits for ^{143}Nd are shown in Table IX, and the parameter values found are listed in Table X along with other relevant information. In Table X, the fourth line gives the parameter values deduced for ^{143}Nd by least-squares fitting expressions (20) and (21) to the corrected values of A and B (listed in Table VI). The first three lines of the table will be discussed in Sec. III L.

It is seen that the five A's can be fitted to within 0.003% with the three-parameter expressions. The value found for a^{12} differs from that for a^{01} by less than 3%, and the contact parameter a^{10} is opposite in sign and less than 3% as large as a^{01} or a^{12}. The three-parameter fit to the five measured B's is good to within 0.2%. The reason the A's are fitted so much better than the B's is not clear but is probably related to the fact that contributions of the type $\langle\psi|\mathcal{H}_{\mathrm{hfs}}|\psi'\rangle$, where $\psi' \neq \psi$, can occur only for the relatively unimportant $\overrightarrow{U}^{(12)1}$ part of the A's, but may occur in all three parts of the B's, including the dominant term $\overrightarrow{U}^{(02)2}$. Thus, the theoretical expressions for the B's may be more sensitive to small components in the eigenvectors.

It may be mentioned that the differences between the observed and calculated B values amount to only 1 or 2 in the fourth significant figure, and the eigenvectors are given[6,20] to only four figures. It is remarkable that the fits are so good when one considers that the eigenvectors span only the single $4f^46s^2$ configuration. The close agreement is probably owing to the capacity of the coefficients $a^{k_s k_l}$ and $b^{k_s k_l}$ to absorb configuration-interaction effects in second order, as shown by Wybourne.[31]

The nonrelativistic part of the quadrupole interaction is dominant (b^{02} is much larger than b^{13} or b^{11}) and is used in Sec. III M to extract the nuclear

TABLE IX. Three-parameter fits to the A and B values observed for five states of ^{143}Nd.

Atomic state	A^{obs}	A^{calc}	$A^{obs}-A^{calc}$	B^{obs}	B^{calc}	$B^{obs}-B^{calc}$
$^5I_4$	−195.652 (1)	−195.653	0.001 (1)	122.595 (17)	122.528	0.067 (17)
$^5I_5$	−153.679 (1)	−153.679	0.000 (1)	115.745 (18)	115.838	−0.096 (18)
$^5I_6$	−130.611 (1)	−130.608	−0.003 (1)	119.291 (23)	119.401	−0.110 (23)
$^5I_7$	−117.604 (1)	−117.607	0.003 (1)	129.291 (24)	128.989	0.302 (24)
$^5I_8$	−110.476 (3)	−110.475	−0.001 (3)	143.952 (87)	144.113	−0.161 (87)

electric-quadrupole moment. In fact, if b^{13} and b^{11} are set equal to zero (the nonrelativistic limit), the single-parameter (b^{02}) expressions will fit all five B's to within 1.5% for b^{02} − 566.0 MHz.

Another way of looking at these data is to use the measured A's and B's for the first four states $^5I_{4,5,6,7}$ to evaluate the $a^{ksk\ell}$ and the $b^{ksk\ell}$, and then to predict A and B for the $^5I_8$ state. The $^5I_8$ A value predicted in this way is within 0.01% of the experimental value (i.e., within four standard deviations) and the B value to 0.7% (12 standard deviations). That the fit to the experimental hfs constants of the first four states (within 1–2 standard deviations) is so much better than that in Tables IX and X for all five states (within 4–12 standard deviations) suggests that the eigenvector for the $^5I_8$ state may not be as accurate as those for the other four. The same conclusion is suggested by the g-factor results of Table II.

The empirically determined parameter values in the fourth line of Table X may be compared with the calculated values (last two lines of the table) obtained by Lewis[10] and by Rosen and Lindgren,[11] who used Hartree-Fock-Slater wave functions and the experimental values[8] for the nuclear moments of ^{143}Nd. The difference between the calculated and experimental values is remarkably small for a^{01}: Lewis's result is 1.4% too small and that of Rosen and Lindgren is 2.5% too large. The value found[32] for a^{01} from the nonrelativistic Hartree-Fock value of $\langle r^{-3}\rangle_{4f}$, for comparison, is 14% too large. It is well known[33] that the ordinary Hartree-Fock procedure commonly overestimates expectation values.

The values calculated relativistically[10,11] for a^{12} and a^{10} are not in such good agreement with the experimental values, probably because of distortion due to configuration interaction. Thus, while a^{12} is expected to be larger than a^{01}, it is found experimentally to be smaller. The calculated values[10,11] of a^{10} are of the correct sign but (60–70)% too large. Whether this is owing to a gross overestimate of the contactlike relativistic contribution of the $4f$ electrons or to neglect of true contact contributions through configuration interaction is difficult to say. Core polarization is expected[34] to be small in the neutral rare-earth atoms. Clearly, the behavior of the relativistic radial wave functions very near the origin is of crucial importance. When a more accurate experimental value for $\mu_I(^{143}\text{Nd})/\mu_i(^{145}\text{Nd})$ becomes available, further investigation of the problem would be important in connection with understanding the apparent hyperfine anomaly.

TABLE X. The hfs radial integrals for ^{143}Nd. The parameters $a^{ksk\ell}$ and $b^{ksk\ell}$ are defined in Sec. III D. The bottom line of the table gives the values calculated theoretically by using the previously reported values of the nuclear moments and the relativistic Hartree-Fock-Slater method. The first four lines give values found by empirical fits of the theory to the experimental results, with the integrals treated as adjustable parameters. The four lines correspond, respectively, to retaining the single largest, the five largest, the 12 largest, and the 19 largest components of the Conway-Wybourne eigenvectors before normalization.

Eigenvector set used	Fraction of strength retained (%)	Magnetic-dipole parameters a^{01} (MHz)	a^{12} (MHz)	a^{10} (MHz)	Largest residual (%)	Electric-quadrupole parameters b^{02} (MHz)	b^{13} (MHz)	b^{11} (MHz)	Largest residual (%)
LS limit	≥96.4	−144.878	−270.032	10.948	0.1	−548.585	−86.597	6.067	0.2
Five component	≥99.8	−140.947	−112.876	0.974	0.2	−557.115	−32.812	15.223	0.14
12 component	≥99.999	−140.584	−136.853	3.166	0.003	−555.307	−36.695	17.816	0.2
19 component	100	−140.583	−136.795	3.154	0.003	−555.321	−36.637	17.795	0.2
Calculated values									
Lewis[a]		−138.6	−149.8	5.36		−545	−56.1	30.2	
Rosen and Lindgren[b]		−144.1	−154.6	5.04		−566			

[a]Reference 10.

[b]Reference 11.

TABLE XI. Ratios of hfs parameter values from Table IX. The bottom three lines give calculated ratios, and the top four give empirical ratios which differ from one another only because of different degrees of truncation of the eigenvectors. The line labeled "19 component" is for the complete Conway-Wybourne eigenvector with no truncation.

Eigenvector set used	Parameter ratio a^{12}/a^{01}	a^{10}/a^{01}	b^{13}/b^{02}	b^{11}/b^{02}
LS limit	1.864	−0.076	0.158	−0.011
Five component	0.801	−0.007	0.059	−0.027
12 component	0.973	−0.023	0.066	−0.032
19 component	0.973	−0.022	0.066	−0.032
Calculated ratios				
Casimir factors	1.006	−0.002	0.024	−0.005
Lewis	1.081	−0.039	0.103	−0.056
Rosen and Lindgren	1.073	−0.035		

Although the magnitude of the calculated quadrupole parameters is subject to an over-all scaling factor (there is no independent precise measurement of Q as there is for μ_I), the relative values can be compared with experiment. It is seen that while Lewis's calculated values of both b^{13} and b^{11} are of the proper sign, their magnitudes are overestimated by about 60%. Part of the problem may be due to the sensitivity of the interactions $\tilde{\tilde{U}}^{(13)2}$ and $\tilde{\tilde{U}}^{(11)2}$ to small impurities in the eigenvectors, and part to the relativistic wave functions.

K. Ratios of Hyperfine-Parameter Values

Table XI lists several ratios of the hfs radial parameters. The upper part of the table gives the empirical results (the fourth line gives the ratios for the complete Conway-Wybourne eigenvectors of Table VII), and the bottom three lines give calculated values. It is seen that, in general, the ratios from parameters calculated[10,11] from the relativistic Hartree-Fock-Slater wave functions are in much better agreement with experiment than are those based on the use of Casimir[35] factors. The latter procedure appears to underestimate the relativistic effects considerably. Both procedures fail to take proper account of configuration interaction.

L. Effect of Truncating Eigenvectors

Virtually any eigenvector that one can write down represents a truncation of the actual physical state of an atom. The Conway-Wybourne[6,20] eigenvectors, which span only a single configuration, nevertheless contain many small terms. It is of interest to see how important some of the smaller components are in accounting for the observed hfs properties of the ^5I states. The first four lines of Tables X and XI are intended as indications of such effects. For the entries in the fourth line, the complete Conway-Wybourne eigenvectors (Table VII) were used, as mentioned above. They list 19 components for $J=4$, 14 for $J=5$, 12 for $J=6$, and seven each for $J=7$ and 8. The results in the third, second, and first lines were obtained by retaining only the 12, 5, and single largest components of the eigenvectors, respectively, and the eigenvectors were then renormalized to unity. Thus, the top line is for the *LS*-limit approximation.

Virtually no change in parameter values is found as the eigenvectors are extended from the first 12 components to the first 19 (only the eigenvectors for the $J=4$ and 5 states are affected). The results for the 5-component eigenvectors are markedly different, however, particularly for a^{12} and a^{10}. This is very surprising when it is noted that these eigenvectors, even before renormalization, retain 99.8% or more of the strength of each state. The *LS*-limit approximation retains 96.4% or more of the strength of the states before renormalization but leads to values of a^{12}, a^{10}, b^{13}, and b^{11} that are off by a factor of 2. That these parameters are *extremely* sensitive to the 3.6% impurities in the states is clear. Even for states very near the *LS* limit, it shows that that retention of only the few leading terms in the eigenvectors cannot be expected to lead to reliable values of the hfs radial integrals.

M. Nuclear Electric-Quadrupole Moments of ^{143,145}Nd

If we put $l=3$ in Eq. (15a), we find

$$b^{02}=(e^2Q/h)\langle r^{-3}\rangle_{02}=(e^2Q/49h)(25R_{++}+18R_{--}+6R_{+-})$$
$$=-555.3\ \text{MHz}, \qquad (26)$$

where we have used the value of b^{02} given for ^{143}Nd in Table IX. Because the relativistic $\langle r^{-3}\rangle_{4f}$ values calculated[10,11] for the dominant $(\tilde{\tilde{U}}^{(01)1})$ term in the dipole interaction are within (1–3)% of experiment, it is reasonable that the corresponding quantity $\langle r^{-3}\rangle_{02}$ for the dominant quadrupole term $(\tilde{\tilde{U}}^{(02)2})$ should also be accurate. The values calculated relativistically for this quantity by Lewis[10] $(4.790a_0^{-3})$ and by Rosen and Lindgren[11] $(4.979a_0^{-3})$ differ by only 3.9%. The mean of the two for ^{143}Nd yields

$$Q=hb^{02}/(4.885a_0^{-3})e^2=-0.483\ \text{b}\ . \qquad (27)$$

This is the apparent value, uncorrected for Sternheimer[36] shielding. Although the shielding factor R_{4f} has not been calculated specifically for Nd I, it does not appear[36] to vary a great deal in the $4f$ shell and is probably about $R_{4f}=+0.13$. Thus, the true quadrupole moment is

$$Q(^{143}\text{Nd})=[1/(1-0.13)](-0.483)=-0.56(6)\ \text{b},$$

where the 10% uncertainty arises primarily from uncertainty in the shielding factor. The quadrupole

moment of ^{145}Nd differs from this by the ratio of the B factors given in Eq. (23). Thus, we have the result

$$Q(^{145}\mathrm{Nd}) = -0.29(3)\ \mathrm{b}\ .$$

IV. SUMMARY AND CONCLUSIONS

In this experiment, the three observables A, B, and g_J have been measured precisely in each of five atomic states for the stable odd-A isotope ^{143}Nd, and in four states for ^{145}Nd. It has been shown that the single-configuration eigenvector set obtained by Conway and Wybourne[6,20] by fitting the excitation energies (an independent fourth observable) are consistent with the measured hyperfine and Zeeman expectation values to a very high order, though not to within experimental error. It is suggested that the eigenvector for the $^5I_8$ metastable state may be less accurate than those for $^5I_{4,5,6,7}$. An investigation of the importance of small components in the eigenvectors showed that even extremely small impurities were significant in understanding details of the hfs observations.

The hyperfine radial integrals obtained by fitting the theoretical expressions to the data are compared with values calculated by nonrelativistic Hartree-Fock[32] and by relativistic Hartree-Fock-Slater[10,11] techniques. Although the nonrelativistic result is in poor agreement with experiment, the relativistic results agree very well for the dominant hfs dipole integral. Agreement is much less satisfactory for the two relativistic quadropule integrals associated with the operators $\overleftrightarrow{U}^{(13)2}$ and $\overleftrightarrow{U}^{(11)2}$, however. A detailed check of the relativistic predictions for the dipole integrals associated with $(\vec{s}\,\overleftrightarrow{C}^{(2)})^{(1)}$ and $\vec{S}$ is not practical because of the difficulty of distinguishing between relativistic and configuration-interaction effects. The dipole-parameter ratios $a^{10}/a^{01} = -0.022$ and $a^{12}/a^{01} = 0.973$ are very close to those reported[37] for the near-neighbor atom Sm I, for which $a^{10}/a^{01} = -0.034$ and $a^{12}/a^{01} = 1.014$.

An apparently large value is found for the hyperfine anomaly, but a final conclusion must await a more precise determination of the moment ratio $\mu_I(^{143}\mathrm{Nd})/\mu_I(^{145}\mathrm{Nd})$. The electric-quadrupole moments of the nuclear ground states of ^{143,145}Nd were obtained.

ACKNOWLEDGMENTS

The authors are grateful to Dr. John Conway of the Lawrence Radiation Laboratory, Berkeley, Calif. for permission to include his corrected set of eigenvectors for the ^5I states of Nd I in this paper, and to Professor B. Bleaney of Oxford University for helpful correspondence on the hyperfine anomaly in ^{143,145}Nd.

---

†Work performed under the auspices of the U. S. Atomic Energy Commission.

[1]P. Schuurmans, Physica 11, 419 (1946).

[2]G. E. M. A. Hassan, Physica 29, 1119 (1963); G. E. M. A. Hassan and P. F. A. Klinkenberg, *ibid.* 29, 1133 (1963).

[3]J. Blaise, J. Chevillard, J. Vergès, and J. F. Wyart, Spectrochim. Acta 25B, 333 (1970); J. Blaise, J. F. Wyart, R. Hoekstra, and P. J. G. Kruiver, J. Opt. Soc. Am. 61, 1335 (1971).

[4]K. F. Smith and I. J. Spalding, Proc. Roy. Soc. (London) A265, 133 (1961).

[5]B. R. Judd and I. Lindgren, Phys. Rev. 122, 1802 (1961).

[6]J. G. Conway and B. G. Wybourne, Phys. Rev. 130, 2325 (1963).

[7]I. J. Spalding, Proc. Phys. Soc. (London) 81, 156 (1963).

[8]K. F. Smith and P. J. Unsworth, Proc. Phys. Soc. (London) 86, 1249 (1965).

[9]Preliminary results were reported by W. J. Childs, Bull. Am. Phys. Soc. 15, 1521 (1970).

[10]W. B. Lewis, in Proceedings of the XVIth Colloque Ampère on Magnetic Resonances and Related Phenomena, Bucharest, Romania, 1970 (unpublished).

[11]A. Rosen and I. Lindgren (private communication).

[12]I. I. Rabi, J. R. Zacharias, S. Millman, and P. Kusch, Phys. Rev. 53, 318 (1938).

[13]J. R. Zacharias, Phys. Rev. 61, 270 (1942).

[14]W. J. Childs, L. S. Goodman, and D. von Ehrenstein, Phys. Rev. 132, 2128 (1963).

[15]W. J. Childs and L. S. Goodman, Phys. Rev. 148, 74 (1966).

[16]L. S. Goodman and F. O. Salter, Rev. Sci. Instr. 37, 769 (1966).

[17]N. F. Ramsey, *Molecular Beams* (Oxford U.P., New York, 1956), pp. 272, 277.

[18]M. H. Prior, A. Dymanus, H. A. Shugart, and P. A. Vanden Bout, Phys. Rev. 181, 1665 (1969).

[19]W. J. Childs, Phys. Rev. A 3, 1195 (1971).

[20]J. G. Conway (private communication).

[21]C. W. Nielson and G. F. Koster, *Spectroscopic Coefficients for the p^n, d^n, and f^n Configurations* (MIT Press, Cambridge, Mass., 1963).

[22]C. Schwartz, Phys. Rev. 97, 380 (1955).

[23]P. G. H. Sandars and J. Beck, Proc. Roy. Soc. (London) A289, 97 (1965).

[24]B. R. Judd, J. Math. Phys. 3, 557 (1962).

[25]W. J. Childs, Phys. Rev. A 2, 1692 (1970).

[26]These expressions follow from the development of Ref. 23; except for the use of Casimir factors (Ref. 35), they are equivalent to the treatment of W. J. Childs and L. S. Goodman [Phys. Rev. 170, 50 (1968)].

[27]R. I. Karaziya, Y. I. Vizbaraite, Z. B. Rudzikas, and A. P. Yutsis, *Tables for the Calculation of Matrix Elements of Atomic Operators* (Akademiya Nauk Lit SSR, Institut Fiziki i Matematiki, Akademiya Nauk SSSR, Vychislitel'nyi Tsentr, Moscow, 1967).

[28]M. Rotenberg, R. Bivins, N. Metropolis, and J. K. Wooten, Jr., *The 3-j and 6-j Symbols* (MIT Press, Cambridge, Mass., 1959).

[29]G. K. Woodgate, Proc. Roy. Soc. (London) A293,

117 (1966).
[30]L. E. Erickson, Phys. Rev. 143, 295 (1966).
[31]B. G. Wybourne, *Spectroscopic Properties of Rare Earths* (Interscience, New York, 1965), pp. 148–152.
[32]J. B. Mann, Los Alamos Scientific Laboratory Report No. LA-3691, 1968 (unpublished).
[33]M. S. Fred, J. Phys. (Paris) Suppl. 31, 161 (1970).
[34]M. B. Bleaney, in *Proceedings of the Third International Conference on Quantum Electronics* (Columbia U. P., New York, 1964), p. 595.
[35]H. B. G. Casimir, *On the Interaction Between Atomic Nuclei and Electrons* (Teyler's Tweede Genootschap, Haarlem, Holland, 1936). The Casimir correction factors are conveniently tabulated by H. Kopfermann [*Nuclear Moments*, translated by E. E. Schneider (Academic, New York, 1958), pp. 445–449].
[36]R. M. Sternheimer, Phys. Rev. 146, 140 (1966).
[37]All the relevant Sm work is summarized by A. Rosen [J. Phys. B 2, 1257 (1969)]. The hfs of Sm is discussed in detail by L. L. Armstrong, *Theory of the Hyperfine Structure of Free Atoms* (Interscience, New York, 1971), Chap. IX.

PHYSICAL REVIEW A VOLUME 6, NUMBER 5 NOVEMBER 1972

Hylleraas-Type Wave Functions for Some Excited Three-Electron *S* States*

Sven Larsson
Quantum Chemistry Group, University of Uppsala, Sweden†
(Received 10 April 1972)

The usefulness of Hylleraas-type wave functions for variational calculation of three-electron excited *S* states is investigated. The four lowest $(1s^2ns)\,^2S$ wave functions for lithium are obtained in the same 57-term basis. The calculated energies are −7.477 82, −7.353 92, −7.318 37, and −7.303 39 a.u. compared to the corrected experimental results −7.478 07, −7.354 10, −7.318 53, and −7.303 55 a.u. The largest part (0.000 15 a.u.) of the discrepancies is due to approximations in the core function. For the lowest ^4S state for lithium a 44-term basis was used with the resulting energy −5.212 40. The wave function was analyzed in terms of natural orbitals and found to exhibit strong $2s3s$-$2p3p$ "near degeneracy." The density for the Li state is significantly correlation contracted in the $3s$ region.

I. INTRODUCTION

Variational trial functions with explicit dependence on the interelectronic distance coordinates were introduced by Hylleraas for the He atom.[1] These kinds of wave functions were also used for the lithium ground state,[2] the H_2 molecule[3] and the metastable $He^-\,^4p^o$ state.[4] Later applications using electronic computers for two-electron[5–7] and three-electron[8–11] atomic ions, the Be ground state,[12–14] and the hydrogen molecule[15] have demonstrated their usefulness for these systems. Hylleraas (Hy) expansions have also been used in the calculation of Bethe-Goldstone-type pair functions in the many-electron theory of atoms and molecules.[12,16,17]

For two-electron atomic ions the original approach of Hylleraas with non-negative powers of r_{12}, r_1+r_2, and r_1-r_2 has been extended to more complicated types of trial functions by Kinoshita,[18] Pekeris,[19] Schwartz,[20] Ermolaev and Sochilin,[21] Frankowski and Pekeris,[22] and others. Contrary to Hy expansions these different methods would lead to very difficult integrals in variational calculations for three or more electrons or in pair function calculations. It is therefore important to keep the Hy form when improving the basis sets. For the two-electron ground state this can be done by choosing some large parameters in the exponent, as is demonstrated in Sec. III.

The $(1s^2ns)\,^2S$ states have been calculated earlier by Öhrn and Nordling [9] and Perkins.[11] The wave functions of Öhrn and Nordling were essentially of the form

$$\psi(1,2,3)=A_3\{\phi(1,2)\varphi(3)\}\,. \tag{1}$$

φ was optimized by variation of the exponential parameters in a three-term basis, whereas ϕ was taken to be a Hy-type function with only one fixed exponential parameter. In this paper we will instead optimize the core function by variation of the exponential parameters of a four-term Hy-type basis. This optimization is carried out for Li^+. The basis for φ is chosen rather large to make possible a description of four valence orbitals. In addition core-valence correlation is included in an efficient way. This calculation is described in Sec. IV.

The $^4S^e$, $^4P^o$, $^4P^e$ states have been calculated by Holøien and Geltman using only even powers of r_{ij}.[8] The cusp conditions of the Coulomb hole are of no importance in this case since all electrons have the same spin. The Coulomb hole exists then only as a slight modification of the Fermi hole, which has a flat bottom.[23] Benefitting from the simplification obtained when using only even powers of r_{ij}, Holøien and Geltman were able to calculate